Int. J. Electrochem. Sci., 13 **(2018)** 4123 – 4138, doi: 10.20964/2018.05.49

International Journal of
ELECTROCHEMICAL
SCIENCE
www.electrochemsci.org

Evaluation of the Modified Extracted Lignin from Wheat Straw as Corrosion Inhibitors for Aluminum in Alkaline Solution

Mohamed M. El-Deeb[1,2,*], *Essam N. Ads*[1,3] *and Jamal R. Humaidi*[1]

[1] Chemistry Department, Faculty of Science, Ha'il University, 81451 Hail, P.O. Box 2440, KSA
[2] Chemistry Department, Faculty of Science, Beni-Suef University, 62511, Beni-Suef, Egypt.
[3] Chemistry Department, Faculty of Science, Zagazig University, Zagazig, Egypt.
[*]E-mail: eldeebm@yahoo.com

Received: 7 February 2018 / *Accepted:* 8 March 2018 / *Published:* 10 April 2018

Extracted lignin from soda pulping of wheat straw agricultural waste is modified and characterized using spectroscopic and thermal analysis. Modified lignin compounds (LG-OH & LG-COOH) are investigated as corrosion inhibitors for aluminum in 1.0 M NaOH compared to their unmodified lignin (LG) using potentiodynamic polarization measurements and morphological characterization. Data show that the modified lignin compounds shift both the corrosion and the open circuit potentials of aluminum to more noble values as well as decrease its corrosion current density (I_{corr}) compared to its values in blank solution. The maximum inhibition efficiency is found to be in case of LG-COOH followed by LG-OH compared to LG. The higher inhibition efficiency of LG-COOH can be explained to its higher active adsorption sites compared to LG-OH and LG. Adsorption of modified lignin compounds on aluminum surface is confirmed using SEM–EDX analysis. The best fit adsorption isotherm is found to be Langmuir adsorption isotherm with physical nature. Thermodynamic parameters indicate endothermic nature of the corrosion process with higher ordered activated complexes in the presence of lignin compounds

Keywords: Modified Lignin, Aluminum, Adsorption, SEM-EDX, Alkaline Solution

1. INTRODUCTION

Aluminum and its alloys are used in many important industrial applications like automotive, aircraft, construction and electrical power generation [1,2]. Their higher corrosion protection is correlated to the formation of the amphoteric passive film that dissolves when exposed to acids or alkaline solutions [3]. Alkaline solution is considered as the most corrosive media for aluminum, due to the presence of the hydroxide ions that dissolves the amphoteric protective film and shifts its potential to more negative values [4]. Aluminum-air batteries and alkaline etching are considered as

the common applications of aluminum that exposed to the alkaline medium [5-7]. The effectiveness of the aluminum applications in the alkaline solutions is depended on its corrosion protection [5].

Synthetic and/or natural compounds containing an active function group and π-electrons are used to protect metals that exposed to different corrosive media. Low cost and friendly environmental natural compounds are of great importance for use as corrosion inhibitors alternative for the synthetic compounds [8]. Lignin is one of the most abundant naturally polymers deposits in the cell wall of plants during cell maturation, and is the by-product of pulping processes and paper industry [9-11]. Lignin structure contains varied range from different function groups such as phenolic-OH, aliphatic-OH, carbonyls, carboxyls [8]. Applications of extracted lignin as an antioxidant and corrosion inhibitors were studied[12-15].

Ultra-filtrated oil palm fronds lignin were investigated as green inhibitors for mild steel in 0.5 M HCl solutions [16]. Data illustrated that, all lignin fractions had exhibited better corrosion inhibitors for mild steel in 0.5 M HCl with the maximum value at 500 ppm (78%) for soda lignin fraction. The adsorption process was found to be physisorption and fitted Langmuir adsorption isotherm. Abu-Dalo et al. [14] studied the protection efficiency of the sulphonated kraft lignin against the corrosion of steel bar grade 60 in water distribution systems. They reported that, the corrosion resistance of steel was enhanced as well as, the pitting potential was shifted to more noble values in the presence of the studied lignin.

Corrosion protection of mild steel in 0.5 M HCl using modified lignin with 2-naphthol and 1,8-dihydroxyanthraquinone was investigated using electrochemical measurements and surface analysis [8]. The data showed, lignin incorporated with 1,8-dihydroxyanthraquinone had good protection action (IE% = 89.96) than lignin incorporated with 2-naphthol (IE% = 84.04) due to its high polarity.

The goal of our work is to modifies the extracted lignin from soda pulping of wheat straw agricultural waste. In addition, to evaluates the modified structures of lignin as corrosion inhibitors for aluminum in alkaline solution in compared to unmodified one using electrochemical and surface analysis measurements.

2. EXPERIMENTAL

2.1. Materials

Wheat straw agricultural wastes are collected from Hail region – Farm in Hoqrosyn (N, 27.73194 - E, 41.91764) with the following composition (w%): 50.69% α-Cellulose, 21.13% lignin, 23.57% hemicellulose, 72.60% hollocellulose, 4.81% ash and 1.20% alcohol-benzene extract. Sodium hydroxide, hydrochloric acid, sulphuric acid, epichlorohydrin , sodium meta periodate, sodium chlorite, acetic acid and ethanol are provided from Merck Chemical Co., (Germany).

Working electrode is made from aluminum rod (area = 1.0 cm^2) with the chemical composition (wt%) as follows: 99.57% Al, 0.31% Fe, 0.07% Si, 0.015% Ti%, 0.0016% Zn, 0.0003% Cr, 0.0019% Mg, 0.0021% Mn and 0.0007 Cu. All solutions are freshly prepared using bi-distilled water.

2.2. Lignin Extraction:

Wheat straw agricultural wastes are pulping using 16% NaOH solution with liquor ratio 1:6 at room temperature for 2 days. Lignin is precipitated from the waste black liquor filtrate of wheat straw pulping using 50% sulfuric acid. Precipitated lignin is purified through dissolving and stirring in distilled water and adjusting the pH to 10 using 20 wt% aqueous solution of NaOH. Then, 10% HCl solution is dropped into the aqueous solution of lignin until precipitation. The precipitated purified lignin is filtered, washed with distilled water, dried at 60 ^{O}C under reduced pressure until constant weight.

2.3. Modification of Lignin:

2.3.1. Hydrolysis:

5g Lignin (LG) is hydrolyzed by refluxing with 1.5 (w/v) HCl solution (liquor ratio, 1:10) for 6 hours. Then the hydrolyzed lignin (LG-OH) is filtered , washed with distilled water and dried at 60 ^{O}C under reduced pressure until constant weight. The acid hydrolysis produced as shown in scheme (1) are in a good agreement with previously reported[17].

2.3.2.Carboxylation:

5g Lignin is refluxed with epichlorohydrin (100 ml) for 3 hours, then filtered, washed with ethanol and water and dried under vacuum at 60 ^{O}C for 12 hour. The obtained cross-linked structure is mixed with 100 ml 10% $NaIO_4$, stirred at room temperature for 24 hour and filtered, wash with distilled water. Then treated with 50 ml 0.4 M NaClO in 2 M acetic acid at room temperature for 48 hour. The carboxylated lignin (LG-COOH) is filtered , washed with distilled water and dried at 60 ^{O}C under reduced pressure until constant weight.

2.4. Characterization of Lignin and its modified compounds:

FT-IR for LG, LG-OH and LG-COOH are carried out using a shimadzu FTIR- 430 Jasco spectrophotometer. TGA are performed with a Shimadzu DT-30 thermal analyzer , from ambient temperature up to 700°C at a rate of 10 °C/min.

2.5. Electrochemical Measurements:

Standard three-electrode cell with working, reference and counter electrodes are Al (1cm^2), Ag/AgCl (saturated) and Pt sheet (1cm^2), respectively is used for the electrochemical measurements. Potentiodynamic measurements are achieved by changing the electrode potential automatically ± 500 mV against the E_{OCP} with scan rate of 10 mVs^{-1}. All electrochemical experiments are performed using the Potentiostat / Galvanostat (AUTOLAB PGSTAT 128N) and NOVA 1.10 software is used for recording and fitting the obtained data. Prior to each experiment, working electrode is polished

successively with fine grade emery papers, cleaned with acetone, washed with bi-distilled water and finally dried.

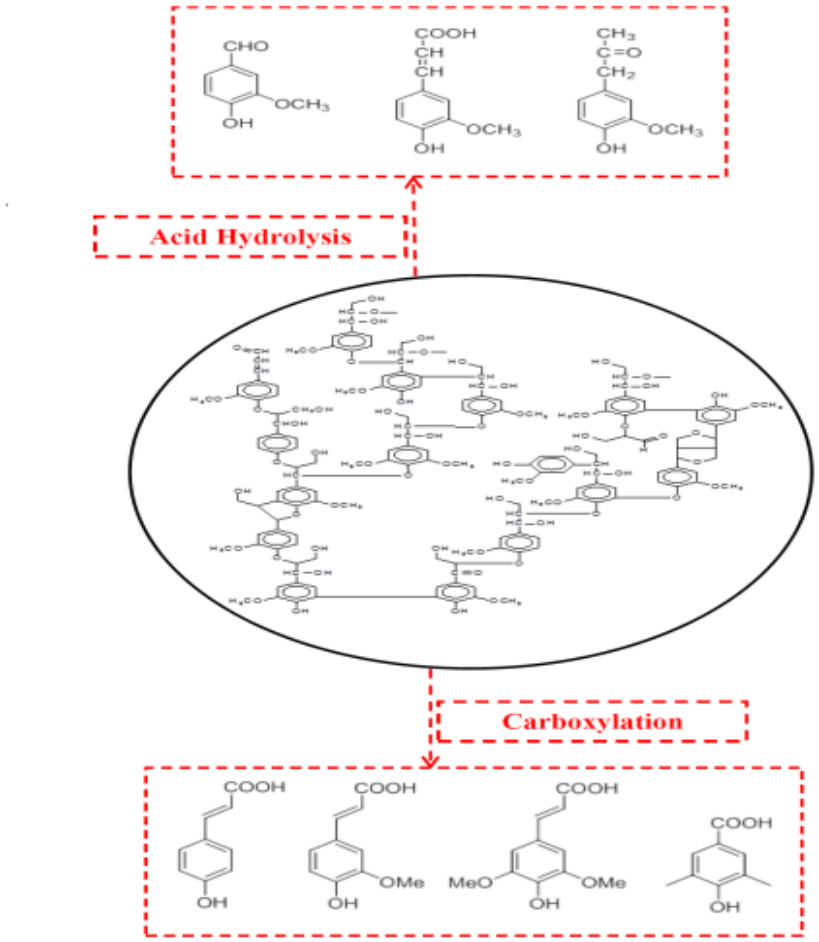

Scheme 1. Route for the modification of lignin

2.6. SEM/EDX Analysis:

Surface analysis is achieved using JSM-6510LA (JEOL, Tokyo, Japan). Prior to the analysis, aluminum specimens are immersed in 1.0 M NaOH for 3 hours in the absence and presence of 300 ppm of the modified and unmodified lignin, then washed and dried.

3. RESULTS AND DISCUSSIONS:

3.1. Spectroscopic characterization of LG, LG-OH and LG-COOH:

3.1.1. FT-IR:

The infrared spectra for LG, LG-OH and LG-COOH are shown in Figure (1). Data show the characteristic bands of aromatic skeleton vibrations appearing at 1594, 1507, 1456, 1421 cm^{-1} for LG

and at 1594, 1510, 1455, 1422 cm^{-1} for LG-OH, while for LG-COOH appears at 1507, 1453, 1394 cm^{-1} [18].

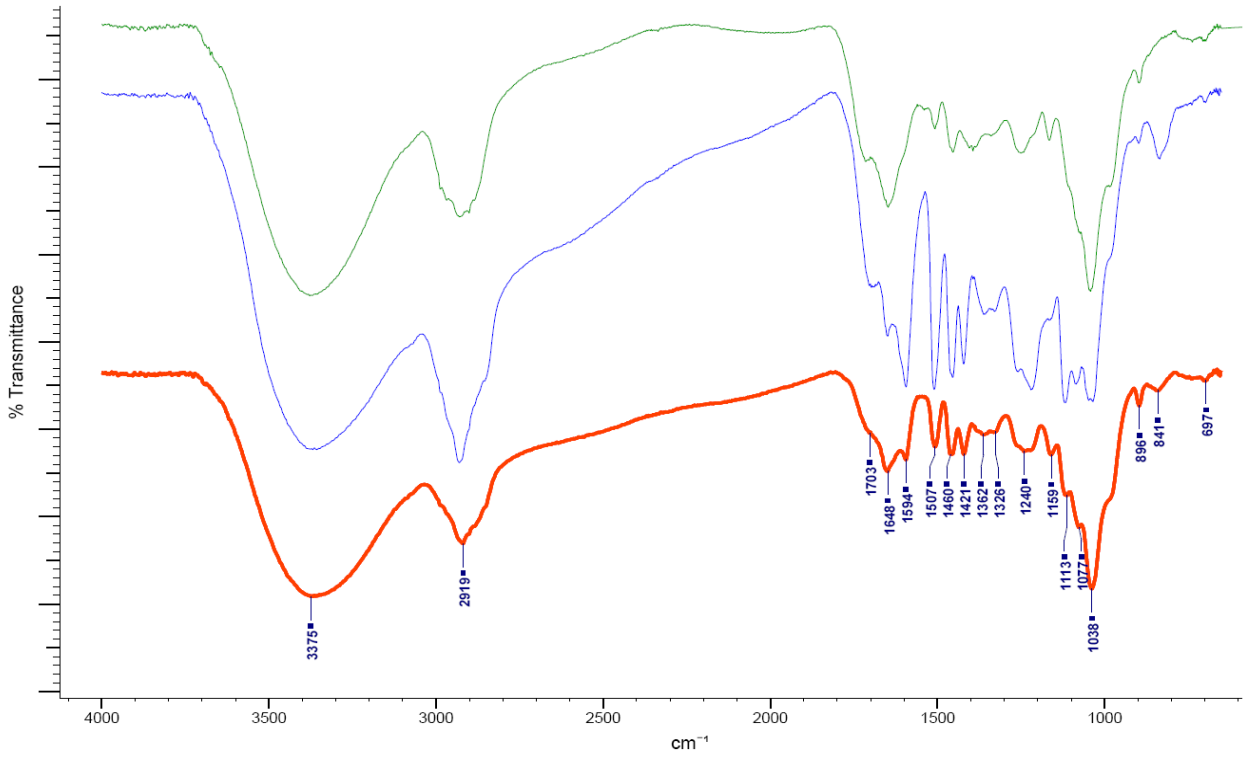

Figure 1. FT-IR spectra of LG, LG-OH and LG-COOH

Medium adsorption band appears at 1703, 1704 and 1715 cm^{-1} for LG, LG-OH and LG-COOH is assigned to the stretching vibration of C=O. The weak absorption band appears at 1113 cm^{-1} for LG and that appears as a medium absorption band at 1117 cm^{-1} for LG-OH (disappears in LG-COOH) can be attributed to β-aryl ether bond in their structures as illustrated in Scheme (1). The weak adsorption band appears at 1160 cm^{-1} and 1165 cm^{-1} for LG and LG-COOH respectively, that disappeared in case of LG-OH can be assigned to C-O stretching in ester groups (c.f. Scheme 1). Other infrared absorption bands and their assignment are summarized in Table (1).

Table (2) shows the relative absorbance (ratio of band intensity of different groups / band intensity at 1325 cm^{-1}) for LG, LG-OH and LG-COOH. It is seen that the relative absorbance of OH phenolic groups at 1375 cm^{-1} in case of LG-COOH is higher than that in LG-OH and LG. This finding is explained to the increase of polar carboxyl groups in LG-COOH structure compared to LG and LG-OH. Also, increasing the degradation of β-O-4 linkage between the units of lignin molecule, increases the OH phenolic groups in LG-OH and LG-COOH structures. On addition, the higher relative absorbance of phenolic OH group band of LG-OH to LG can be correlated to the possibility of cleavage of β-aryl ether [19], that can be confirmed by the decreasing in the relative absorbance of β -aryl ether link band at 1119 cm^{-1} of LG-OH, as a result to the acidolysis of lignin with HCl. The

relative decreasing in the OH absorbance vibration bands of CH_3O- at 2930, 2825, 1454 and 1422 cm^{-1} is attributed to the hydrolysis of methoxy group to phenolic OH groups. This can be illustrated by the increasing the relative absorbance compared with the LG.

Table 1. Infrared absorption bands and their assignments for LG, LG-OH and LG-COOH

Assignments	Wavenumber /cm^{-1}		
	LG	LG-OH	LG-COOH
OH stretching	3368	3357	3370
C-H stretching	2919	2930	2930
C=O of carboxyl group	1703	1704	1715
C=O of conjugated carbonyl stretching	1648	1649	1647
Aromatic skeletal vibrations	1594 1507 1456 1421	1594 1510 1455 1422	1539 1507 1453 1394
Syringyl ring breathing with C–O stretching	1325	1358	1394
Aromatic C–O stretching	1230	1220	1242
β -aryl ether bond	1113	1117	-------
C–O stretch in ester groups	1160	-------	1165
Aromatic C–H in-plane deformation for guaicyl type	1039	1035	1042
Aromatic C–H out of plane bending	896 840	895 836	896 738

Table 2. Relative absorbance (ratio of band intensity of different groups / band intensity at 1325 cm^{-1}) of some characteristic bands of LG, LG-OH and LG-COOH

	OH (3368 cm^{-1})	**OH Phenolic (1375 cm^{-1})**	**COOH (1715 cm^{-1})**	**β-o-4 lignin (1112 cm^{-1})**	**CH aromatic ring (1600 – 1605 cm^{-1})**	**CH stretching (2920 cm^{-1})**
LG	4.13	0.93	1.00	2.13	1.57 1.78	3.11
LG-OH	1.80	1.03	0.88	1.52	1.41 1.12	1.89
LG-COOH	0.27	1.17	1.25	1.13	0.76 1.67	1.52

The intensity of the broad OH band is seen to decrease relatively to the intensity of CH vibration of methoxy group from LG to LG-OH and LG-COOH. This observation indicates that, LG undergoes oxidation and formation of hydroxyl groups or ring cleavage leading to lactones structure as shown in scheme (1), which compatible with previously reported [20].

Moreover LG-COOH has more carboxylic groups and more cleavage of β-O-4 linkage between the units of phenyl propane unites (LG molecule)than that in case of LG-OH and LG. This hypothesis is confirmed by the higher relative absorbance of (C=O in carboxylic groups at 1715 cm^{-1} / band intensity at 1325 cm^{-1}) as well as the lower relative absorbance of the characteristic band of β-O-4 of LG-COOH than the LG-OH and LG. The relative absorbance of hydroxyl group bands of LG-OH is lower than that in case of LG as showed in Table (2).

The relative absorbance of CH vibration of the aromatic ring at 1600 cm^{-1} is lower than that at 1507 cm^{-1} referred to the transformation of the guaicyl type lignin to the syringyl type of LG-COOH and peroxyacetice acid lignin [21].

3.1.2. Thermal Analysis

Lignin derivatives are characterized by TGA that used to determine the thermal stability and reveal the weight loss % of materials with respect to the temperature. Lignin structure is composed of mostly aromatic rings with different branches, these chemical bonds lead to a broad temperature range of degradation from 200 to 700 ^oC [17, 22]. About 35 to 40 wt % of all lignin derivatives still remained unvolatized (Char residues) at nearly 700 ^oC , which is due to the formation of highly condensed aromatic structures that form char as tabulated in Table (3).

The decomposition of these compounds started from 39 ^oC and the weight loss (%) values are observed as 8.5, 5.3 and 7.09% for LG, LG-OH and LG-COOH respectively, which assigned to water evaporation. In the temperature range between 135 and 414 ^oC, weight loss (%) ranges are between 20.3 - 46.5% because of degradation of carbohydrates. In the final degradation is found to be in temperature range between 400 to 700 ^oC. The weight loss (%) values are 33.7, 13.3 and 53.8 %, that can be attributed to the removal of the gaseous products. The gaseous products are produced due to the presence of phenols, alcohols, aldehydes and acids. Data of Table (3) clearly show that, LG-COOH has the greatest thermal stability and highest char yield of 39.1% compared to LG (37.4 %) and LG-OH (34.9 %).

Table 3. Thermal gravimetric analysis of LG, LG-OH and LG-COOH

Sample	Minor decomposition temperature (^oC)	Wt. Loss (%)	Major decomposition temperature (^oC)	Wt. Loss (%)	Char yield (%)
LG	182.5	8.6	701.2	62.6	37.4
LG-OH	135.5	5.3	698.9	65.1	34.9
LG-COOH	188.0	7.1	689.6	60.9	39.1

3.2. Open circuit potentials (E_{ocp}) measurements:

Changes in the open circuit potentials (E_{OCP}) values of Al in 1.0 M NaOH in the absence and presence of different concentrations (50 – 300 ppm) of LG, LG-OH and LG-COOH at 30 ^{o}C with scan rate of 10 mVs^{-1} are shown in Figure (2). Data clearly show, the values of E_{OCP} of Al in the presence of the studied compounds are shifted towards more positive potentials comparing with its values in the blank solution. These results demonstrate the effect of these compounds on reducing the vigorous anodic dissolution of Al in alkaline solution. This effect is correlate to their adsorption on Al/NaOH interface and forming a barrier protective film, that blocks the active sites in Al surface [23].

The vigorous open circuit alkaline dissolution of Al in 1.0 M NaOH is explained to the formation of soluble aluminate ($[Al(OH)_4]^-$) as previously reported [1, 24] as follows:

Anodic reactions

$$Al + 3OH^- \longrightarrow Al(OH)_3 + 3e^- \quad (1)$$

Formation of soluble aluminate

$$Al(OH)_3 + OH^- \longrightarrow [Al(OH)_4]^- \quad (2)$$

Cathodic reaction:

$$2H_2O + 2e^- \longrightarrow H_2 + 2OH^- \quad (3)$$

Overall reaction

$$2Al + 2OH^- + 6H_2O \longrightarrow 2[Al(OH)_4]^- + 3H_2 \quad (4)$$

The positive shift increases with increasing the concentrations of all studied compounds with the following order: LG-COOH > LG-OH > LG. This trend supports the postulate of highly covered area of Al surface by adsorbed LG-COOH layers compared to LG and LG-OH that increase its efficiency as a barrier film on the Al/NaOH interface. Presence of plenty adsorption centers in LG-COOH structure as shown in scheme (1), reinforces the above hypothesis that be confirmed by the calculated both the inhibition efficiencies and the adsorption energies

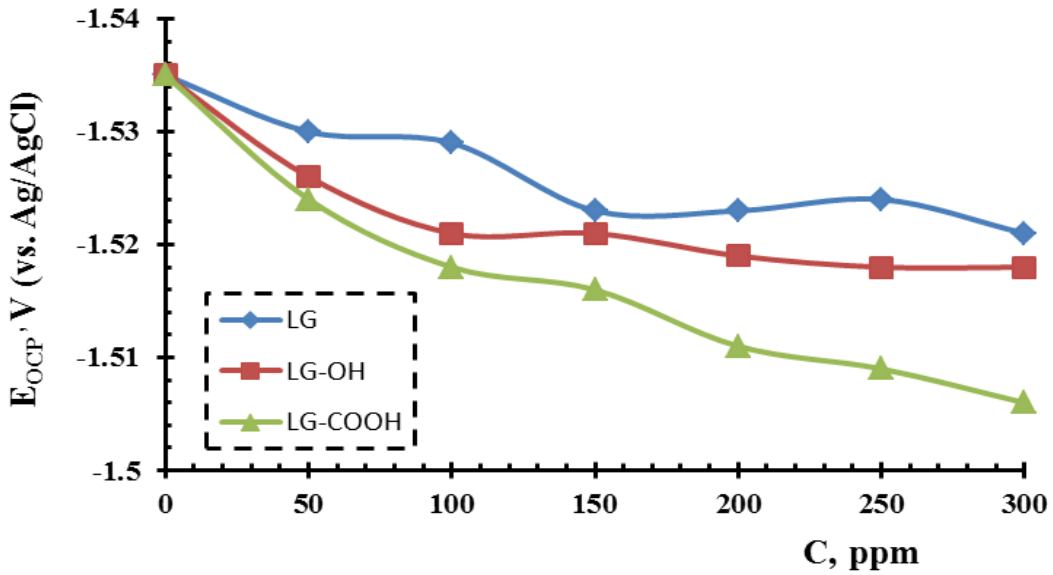

Figure 2. Variation of E_{OCP} with LG, LG-OH and LG-COOH concentrations (ppm), based on potentiodynamic polarization measurements at 30^{o}C with scan rate of 10 mVs^{-1}.

3.3. Potentiodynamic polarization measurements:

Potentiodynamic polarization measurements of Al in 1.0 M NaOH solution are performed by changing its potential automatically ± 500 mV against the E_{OCP} in the absence (Blank solution) and presence of different concentrations (50 – 300 ppm) of LG, LG-OH and LG-COOH at 30 ^{o}C with scan rate of10 mV/s. Figure (3) shows the *E/I* curves of Al in 1.0 M NaOH in the presence of 300 ppm of the studied lignin compounds while its electrochemical parameter derived from Tafel polarization curves in the concentrations range between 50 to 300 ppm are tabulated in Table (4). Results show that, the presence of the studied lignin compounds shifts the corrosion potential (E_{corr}) of Al to more positive values as well as, decreases its corrosion current density (I_{corr}) compared to its values in blank solution. These results are attributed to their protective and inhibitive effect against the vigorous alkaline dissolution of Al. Their protective effect is correlated to their adsorption on Al surface and formation of the protective layer in Al/NaOH interface as discussed before. The maximum calculated inhibition efficiency [25] for LG, LG-OH and LG-COOH is recorded at 300 ppm with the following order: LG < LG-OH < LG-COOH. This relation can be explained to the increase in the number of adsorbed inhibitor molecules on Al active sites and consequently, an increase in its surface that be covered by these compounds. In addition, the effect of the studied lignin compounds on the mechanistic anodic and cathodic corrosion reaction can be understood from Tafel plots [26,27]. It is noted from Figure (3) and Table (4) that both the anodic and cathodic Tafel curves are shifted to lower current density regions compared to their values in the blank solution. This observation indicates the mixed type inhibitors, which reduce and block both anodic and cathodic active reaction on Al surface sites. The higher inhibition efficiency of LG-COOH can be explained to its higher active adsorption sites compared to LG-OH and LG as concluded from scheme (1).

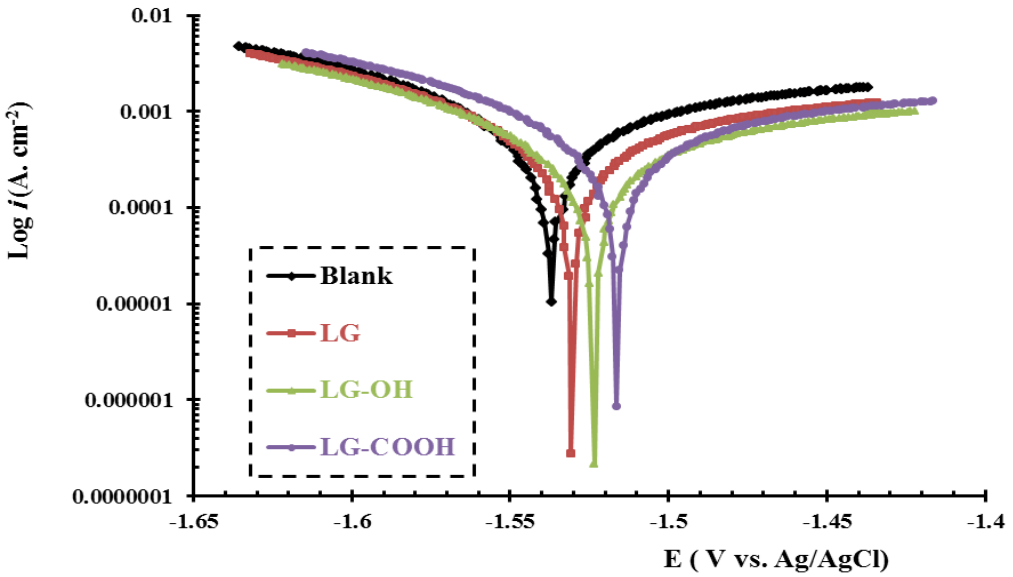

Figure 3. Potentiodynamic polarization plots of Al in 1.0 M NaOH solution in the absence and presence of 300 ppm of LG, LG-OH and LG-COOH at 30 °C in the potential range ± 500 mV against the E_{OCP} with scan rate of 10 mV/s.

Table 4. Electrochemical kinetic parameters and inhibition efficiency of aluminum in 1.0 M NaOH solution in the absence and presence of different concentrations of lignin compounds at 303 K

C, ppm		E_{corr} *(V) (vs. Ag/AgCl)*	I_{corr} *(mA.cm^{-2})*	βa (mV. dec^{-1})	βc (V. dec^{-1})	θ	*IE%*
Blank		-1.536	3.92	234.8	-1.298	--	--
LG	50	-1.532	2.79	204.13	-0.772	0.288	28.8
	100	-1.529	2.23	177.82	-1.324	0.431	43.1
	150	-1.525	1.51	165.91	-1.65	0.615	61.5
	200	-1.523	1.20	167.65	2.57	0.694	69.4
	250	-1.518	1.13	162.28	1.73	0.711	71.1
	300	-1.513	1.01	139.74	0.691	0.742	74.2
LG-OH	50	-1.531	1.71	173.57	1.406	0.563	56.3
	100	-1.528	1.54	163.32	1.69	0.607	60.7
	150	-1.523	1.35	158.08	1.01	0.656	65.6
	200	-1.520	1.16	140.13	0.551	0.704	70.4
	250	-1.516	1.08	140.47	0.644	0.724	72.4
	300	-1.511	0.98	135.87	0.598	0.747	74.7
LG-COOH	50	-1.531	1.65	172.95	-2.19	0.579	57.9
	100	-1.526	1.30	156.28	0.784	0.668	66.8
	150	-1.527	1.09	153.06	1.16	0.722	72.2
	200	-1.518	0.98	151.33	0.507	0.750	75.0
	250	-1.512	0.86	146.25	0.282	0.781	78.1
	300	-1.508	0.74	130.05	0.434	0.811	81.1

3.4. Adsorption Isotherms:

The mechanism of the inhibition efficiencies for LG, LG-OH and LG-COOH is explained to the adsorption of these compounds on Al surface. Adsorption process can be classified into chemically or physically in its nature. Therefore, the experimental data are fitted to several adsorption isotherms at 30 ^{o}C to understand the adsorption behavior of lignin compounds on Al surface. The best fit is acquired to be with Langmuir adsorption isotherm which assumes that a solid surface contains a fixed number of adsorption sites and each site holds one adsorbed species (c.f. Figure 4) [28]. Calculated

values of the equilibrium adsorption constant (K_{ads}) for LG, LG-OH and LG-COOH based on Langmuir adsorption isotherm [29] are tabulated in Table (5). Furthermore, their standard free energies of the adsorption (ΔG^{o}_{ads}) that be calculated from equation (5) [30] are listed in Table (5).

$$\Delta G^{o}_{ads} = -RT\ln(1x10^{6} K_{ads}) \quad (5)$$

where R is the universal gas constant, T is the absolute temperature, and the value $1x10^{6}$ is the concentration of water (mg/L) in the solution.

Table 5. Thermodynamic parameters of the adsorption process based on the Langmuir adsorption isotherm calculated from potentiodynamic polarization measurements at 303 K

Inhibitor	K_{ads}, $(ppm)^{-1}$	ΔG^{o}_{ads}, (kJ/mol)
LG	0.0079	-22.6
LG-OH	0.0277	-25.2
LG-COOH	0.0289	-25.9

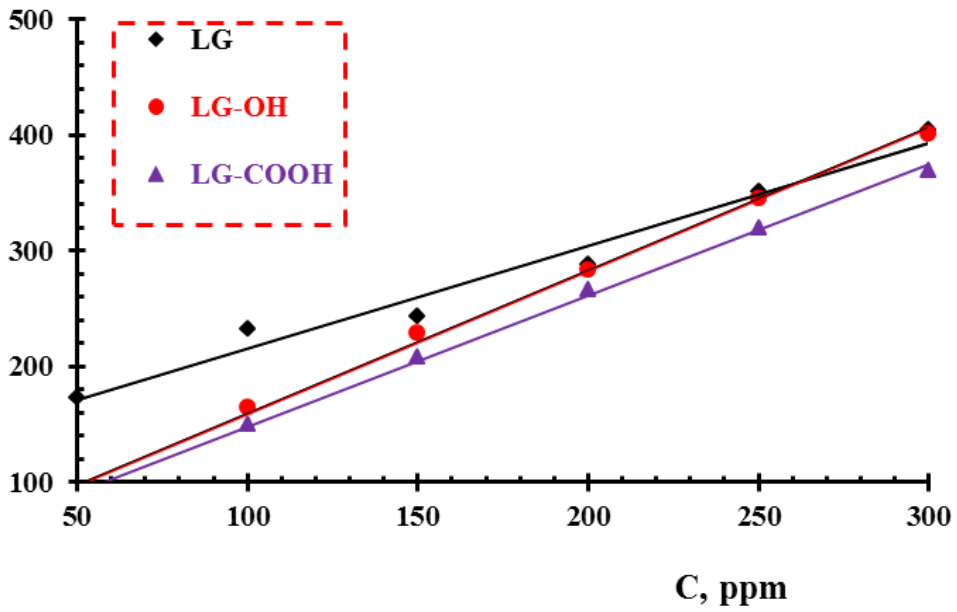

Figure 4. Langmuir adsorption isotherm based on potentiodynamic polarization Measurements at 303 K

It is reported that the ΔG^{o}_{ads} values of around -20 and -40 kJ mol^{-1} , suggesting physical and chemical adsorption process respectively [30]. It can be noticed from the values of ΔG^{o}_{ads} and K_{ads} that, the adsorption process is spontaneous and physically in its nature for all lignin compounds. The more negative value of ΔG^{o}_{ads} and the higher value of K_{ads} are recorded to LG-COOH, that supports its higher inhibition efficiency compared to LG-OH and LG, as a result of the higher active adsorption centers within its structure as discussed before. The order of the calculated ΔG^{o}_{ads} and K_{ads} is in a good

agreement with the order of the inhibition efficiencies that be calculated from the potentiodynamic polarization measurements.

3.5. Surface Morphology:

SEM images of Al surface immersed in 1.0 M NaOH solution for 3 hours in the absence and presence of 300 ppm of LG, LG-OH and LG-COOH at 30 ^{o}C are given in Figure (5). The micrograph of Al in the absence of lignin compounds (blank) shows, clear pits and cavities with high degree of roughness as a result of vigorous damage by the attack of NaOH. On the other hand, addition of lignin compounds to the corrosive medium, decreases the Al surface roughness as well as its surface homogeneity increases with the following order : LG < LG-OH < LG-COOH. This enhancement in both the roughness and the homogeneity of Al surface is explained to the adsorption of these compounds on Al surface that, forms a barrier protective layer from an aggressive attack by NaOH solution [2]. Adsorption of lignin compounds on Al surface is confirmed by the appearances of the characteristic peak for C in the elemental composition obtained from the SEM–EDX analysis and the surface composition is shown in Figure (5).

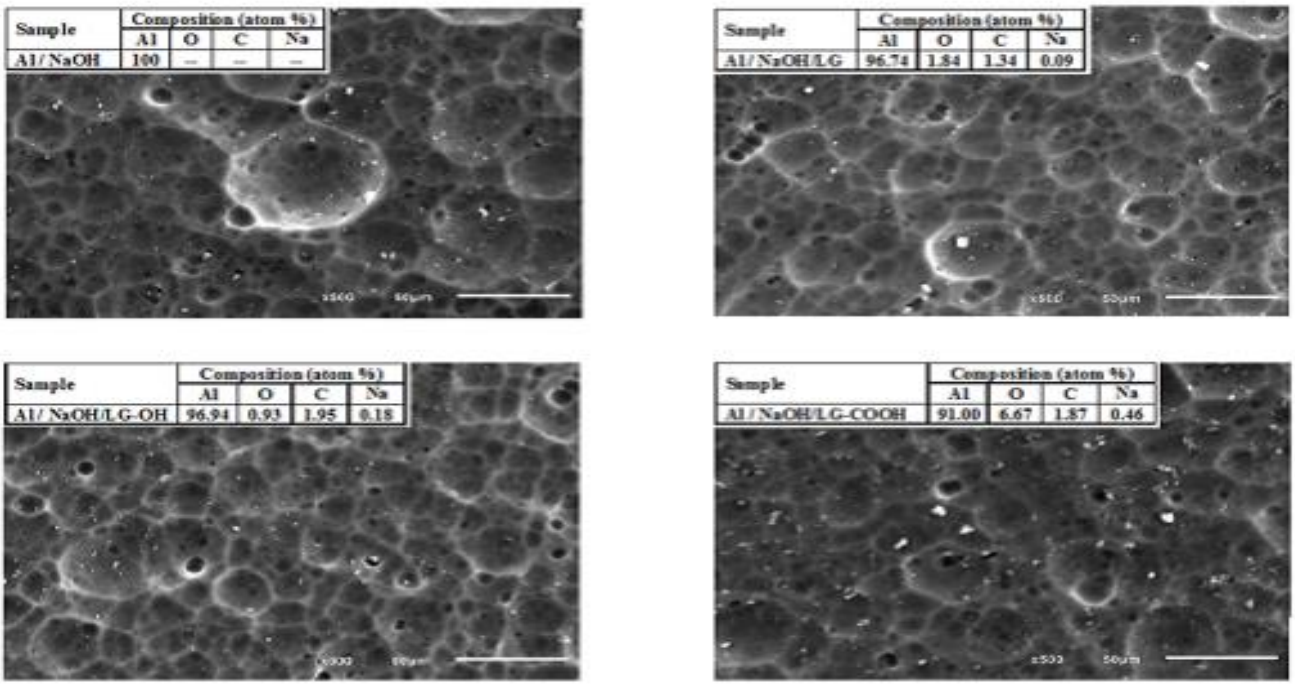

Figure 5. SEM images and surface composition of Al surface exposed to 1.0 M NaOH in the absence and presence of 300 ppm LG, LG-OH and LG-COOH at 30 ^{o}C for 3 hours.

3.6. Effect of temperature:

Effect of temperature on the potentiodynamic polarization behavior of Al in 1.0M NaOH solution is studied in the absence and presence of 300 ppm of LG, LG-OH and LG-COOH, with a scan rate of

10 mVs^{-1} at 303, 313, 323 and 333 K and its electrochemical parameters and the calculated inhibition efficiencies are tabulated in Table (6).

Table 6. Electrochemical kinetic parameters and inhibition efficiency of aluminum in 1M NaOH solution in the absence and presence of 300 ppm lignin compounds at different temperature

T, K	$-E_{corr}$ (V vs. Ag/AgCl)				I_{corr} ($mA.cm^{-2}$)				E_a (kJ/mol)				ΔH^* (kJ/mol)				ΔS^* (J/mol.K)			
	Blank	LG	LG -OH	LG - COOH	Blank	LG	LG -OH	LG - COOH	Blank	LG	LG -OH	LG - COOH	Blank	LG	LG -OH	LG - COOH	Blank	LG	LG -OH	LG - COOH
303	1.536	1.513	1.511	1.508	3.92	1.01	0.98	0.74	21.2	50.9	51.6	58.1	18.4	48.6	49.2	54.9	-172.7	-84.3	-83.0	-66.0
313	1.536	1.524	1.520	1.510	5.71	1.99	1.78	1.58												
323	1.538	1.532	1.528	1.517	6.80	3.72	3.31	3.16												
333	1.540	1.533	1.530	1.522	8.65	6.32	6.31	5.98												

It is observed from the data that, increasing the solution temperature shifts the corrosion potentials (E_{corr}) of Al toward more negative values and increases its corrosion current densities (I_{corr}). Furthermore, decreasing the inhibition efficiencies of the studied lignin compounds with raising the solution temperature; supports the physical adsorption nature of these compounds on Al surface.

Thermodynamic activation parameters (Ea, ΔH^o, ΔS^o) of Al dissolution in 1.0 M NaOH solution in the absence and presence of 300 ppm of LG, LG-OH and LG-COOH are calculated using Arrhenius and transition state equations. Figure (6) represents the relation between log (CR ~ I_{corr}) and 1/T, the values of E_a are calculated and tabulated in Table (6) from the slope of the following Arrhenius equation [31]:

$$\text{Log (CR} \sim I_{corr}) = \text{Log A} - Ea/2.303\ RT \quad (6)$$

where CR is the corrosion rate and is directly to the corrosion current density (I_{corr}) [1,32], E_a is the apparent activation energy, A is the pre-exponential factor, T is the absolute temperature and R is the ideal gas constant. It is clear that the addition of lignin compounds to the alkaline dissolution of Al, increases its activation energy of dissolution. This means that the adsorption of lignin compounds on Al surface leads to the formation of barrier layer that retards the metal dissolution. Moreover, the order

of the increasing in the activation energies follows the following order: LG < LG-OH < LG-COOH, that agree well with the order of the inhibition efficiency of the studied compounds.

The activation enthalpy (ΔH^*) and activation entropy (ΔS^*) of the dissolution process are calculated from the following equation [33]:

$$\text{Log (CR} \sim I_{corr} / T) = (\text{Log } R/hN) + \Delta S^* / 2.303\ R - \Delta H^* / 2.303\ RT \quad (7)$$

where *T* is the absolute temperature, *R* is the ideal gas constant, h is Plank's constant and N is Avogadro's constant

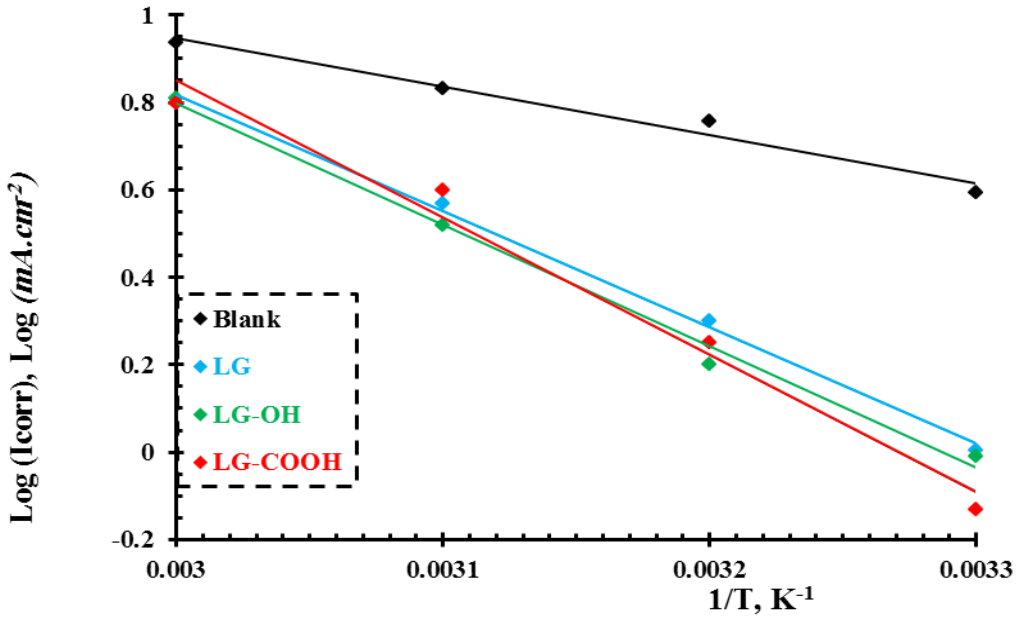

Figure 6. Arrhenius plots based on potentiodynamic polarization measurements at 300 ppm.

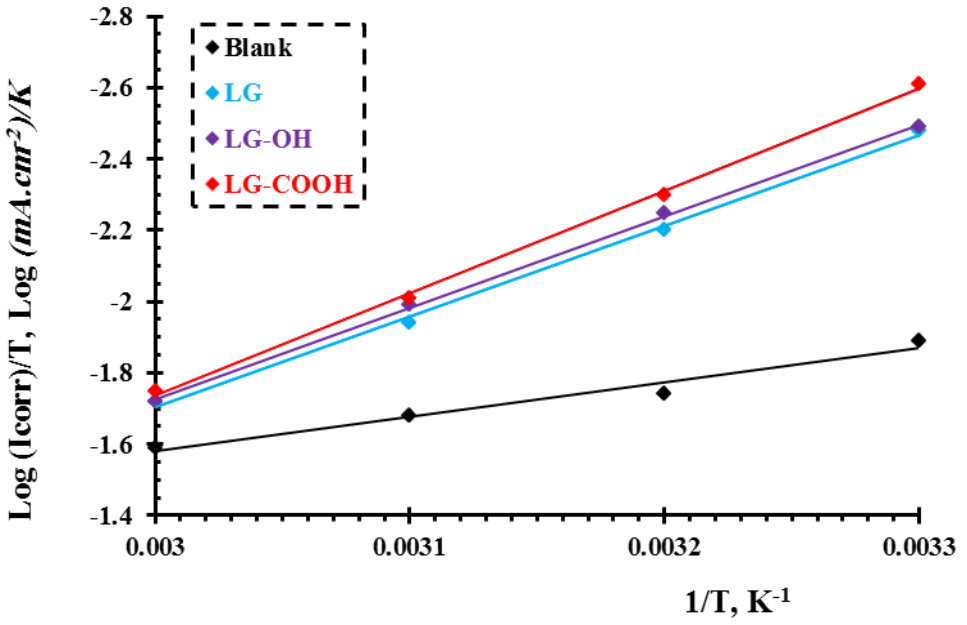

Figure 7. Transition state plots based on potentiodynamic polarization measurements at 300 ppm.

Figure (7) represents a straight lines obtained from the relation between log (I_{corr}/T) and 1/T, from which the values of ΔH^* and ΔS^* will be calculated and given in Table (6). Data clearly show that the corrosion process of aluminum dissolution in 1.0 M NaOH is endothermic nature with higher ordered activated complexes in the presence of lignin compounds compared to blank solution.

4. CONCLUSION

1. Extracted lignin from soda pulping of wheat straw agricultural waste is modified and characterized using spectroscopic and thermal analysis as well as evaluated as corrosion inhibitors for aluminum in 1.0 M NaOH.
2. Potentiodynamic polarization measurements reveal that the modified lignin compounds are good inhibitors and their inhibition efficiencies increase with increasing the concentrations.
3. Mechanism of their inhibition is correlated to their physical adsorption on aluminum surface and fits Langmuir adsorption isotherm.
4. The micrograph of aluminum surface shows, clear pits and cavities with high degree of roughness, while the addition of lignin compounds to the alkaline medium decreases its roughness.
5. Thermodynamic parameters indicate endothermic nature of the corrosion process with higher ordered activated complexes compared to blank solution .

ACKNOWLEDGEMENT
This project is funded by the Deanship of Scientific Research, University of Ha'il, Kingdom of Saudi Arabia (Project Number: 0150105).

References

1. M. Abdallah, E. M. Kamar, S. Eid and A. Y. El-Etre, *J. Mol. Liq*., 220(2016)755.
2. M. M. El-Deeb, H. M. Alshammari and S. Abdel-Azeim, *Can. J. Chem*., 95(2017)612.
3. T. Hurlen, H. Lian, O. S. Ogegrd and T. V. Valand, *Electrochim. Acta* 29(1984)579.
4. O. K. Abiola and J. O. E. Otaigbe, *Corros. Sci*. 50(2008)242.
5. D. R. Egan, C. Ponce de León, R. J. K. Wood , R. L. Jones, K. R. Stokes and F. C. Walsh, *J. Power Sources* 236(2013)293.
6. Y. Ma, X. Zhou, G. E. Thompson and P. Skeldon, *Corros. Sci*. 66(2013)292.
7. S. S. Golru, M. M. Attar and B. Ramezanzadeh, *Prog. Org. Coat*. 87(2015)52.
8. M. H. Hussin, A. Abdul Rahim, M. Ibrahim and N. Brosse, *Mat. Chem. Phys*. 163(2015)201.
9. D. Fengel, G. Wegener, Wood-Chemistry, Ultrastructure Reaction, Walter de Gruyter, Germany, 1989.
10. K. J. Moore and H. –J. G. Jung, *J. Ranage* 54(2001)420.
11. M. Vagin, S. A. Trashin and A. A. Karyakin, *Electrochem. Commun*., 8(2006)60.
12. R. El Hage, D. Perrin and N. Brosse, *Nat. Resour*. 3 (2012) 29e34.
13. M. H. Hussin, A. A. Rahim, M. N. Mohamad Ibrahim, M. Yemloul, D. Perrin and N. Brosse, *Ind. Crop. Prod.* 52 (2014) 544e551.
14. M. A. Abu-Dalo, N. A. F. Al-Rawashdeh and A. Ababneh, *Desalination* 313 (2013) 105e114.

15. Q. Lu, M. Zhu, Y. Zu, W. Liu, L. Yang, Y. Zhang, X. Zhao, X. Zhang and W. Li, *Food Chem*. 135 (2012) 63e67.
16. M. H. Hussin, A. Abdul Rahim , M. N. Ibrahim and N. Brosse, *Measurement*, 78 (2016) 90.
17. A. M. A. Nada, H. AbouYousef and S. El-Gohary, *J. Thermal analysis and Calorometry*, 68 (2002) 265.
18. N. B. Clthup, L. H. Daly and S. E. Wiberley, Introduction to infrared and raman spectroscopy, Academic Press limited,London,1990.
19. K. Landquist, Acidolysis methods in lignin chemistry, (S. Y. Lin and C. W. Dence (Eds), Springer, Berlin 1992, p. 291.
20. A. M. A. Nada, M. El-Sakhawy and S. Kamel, *Polym. Degrad. Stab*.,60(1998)247.
21. A. Seisto and K. Poppius-Levlin, 8th ISWPC Conf. Jun. 6.9, Finland, Helsinki 1995.
22. E. N. Ads, A. M. A. Nada and A. M. El-Masry, *J. Korean Chem. Soc*.,55(2011)86.
23. R. Yildiz, *Corros. Sci*., 90(2015)544.
24. I. Zaafarany, *Port. Electrochim. Acta*, 30(2012)419.
25. S. S. Abd El-Rehim, S. M. Sayyah, M. M. El-Deeb, S. M. Kamal and R. E. Azooz, *Int. J. Ind. Chem*., 7(2016)39.
26. N. K. Gupta, M. A. Quraishi, C. Verma and A. K. Mukherjee, *RSC Adv*., 6(2016)102076.
27. Y. Meng, W. Ning, B. Xu, W. Yang, K. Zhang, Y. Chen, L. Li, X. Liu, J. Zheng and Y. Zhang, *RSC Adv*., 7(2017)43014.
28. P. Singh, M. A. Quraishi and E. E. Ebenso, *Int. J. Electrochem. Sci*., 9(2014)4900.
29. M. M. El-Deeb and S. M. Mohamed, *J. Appl. Polym. Sci*., 122(2011)3030.
30. X. Luo, X. Pan, S. Yuan, S. Du, C. Zhang and Y. Liu, *Corros. Sci*., 125(2017)139.
31. S. S. Abd El Rehim, S. M. Sayyah, M. M. El-Deeb, S.M. Kamal and R. E. Azooz, *Mat. Chem. Phys*., 123 (2010)20.
32. O. L. Riggs Jr. and R. M. Hurd, *Corros*., 23 (1967) 252.
33. M. M. El-Deeb, S. M. Sayyah, S. S. Abd El-Rehim and S. M. Mohamed , *Arb. J. Chem*., 8(2015)527.